The Korean Journal of Ceramics, **2** [1] 11-18 (1996)

Effects of Microstructure on Thermoelectric Properties of $FeSi_2$

Joon Young Choi, Tae Ho Song, Hong Lim Lee and Chul Hoon Pai*

Dept. of Ceram. Eng., Yonsei Univ., 134 Shinchon-dong, Sudaemoon-ku, Seoul 120-749, Korea
**Dept. of Mater. Eng., Univ. of Inchon, 177 Dohwa-dong, Nam-ku, Inchon 402-749, Korea*
(Received August 28, 1995)

The variation of electrical conductivity and Seebeck coefficient of $FeSi_2$ according to the density of the specimen has been observed over the temperature range 50 to 700°C.A conventional pressureless sintering method with various sintering time (0, 0.5, 1, 5 h) at 1190°C and/or various sintering temperatures (1160, 1175, 1190, 1200°C) for 2 h was carried out to prepare $FeSi_2$ specimens having various densities. The relationship between the electrical conductivity and Seebeck coefficient was investigated after two steps of annealing (at 865°C and then 800°C for total 160 h) and thermoelectric measurement. The electrical conductivity for the specimens showed a typical tendency of semiconductor, the average activation energy of which in the intrinsic region (above 300°C) was observed approximately as 0.452 eV, and increased slightly with density. On the other hand, the specimen of the lower density showed the higher value of Seebeck coefficient in the intrinsic region. As the temperature fell into the non-degenerate region, the highly densified specimen which had relatively little residual metal phase showed the higher value of Seebeck coefficient. The power factor of all specimens showed the optimum value at 200°C However, the power factor of the specimen of the lower density increased again from 400°C and that of the higher dense specimen increased from 500°C. The power factor was more affected by Seebeck coefficient than electrical conductivity over all temperature range.

Key words : $FeSi_2$, Seebeck coefficient, Electrical conductivity. Density. Power factor

I. Introduction

Thermoelectric energy conversion utilizing nuclear heat sources has been employed for several decades to generate power for deep space probes. The development decades ago of thermoelectric materials has recently been resurrected in a fury of activity once again for high-temperature thermoelectric power generation. For effective utilization of solar heat, nuclear energy and waste heat from industries, materials possessing high thermoelectric energy conversion efficiencies and usable at high temperatures are intensely required.

The goodness of a semiconductor in thermoelectric conversion is given by its so-called figure of merit, Z, and is expressed[1] by

$$Z = \frac{\sigma\alpha^2}{k} \quad (1)$$

where σ is the electrical conductivity, α the Seebeck coefficient and k the thermal conductivity. For developing thermoelectric materials, a large number of work have been concentrated on increasing the figure of merit, Z by increasing the electrical conductivity and Seebeck coefficient with reduction of thermal conductivity.

Generally, the thermoelectric materials can be classified into three classes by the temperature range, in which the maximum value of figure of merit can be obtained; the low (r.t.~100°C), middle (200~600°C) and high (above 700°C) temperature materials.[2] Iron disilicide, β-$FeSi_2$, attracts an increasing interest as a candidate for base material of thermoelectric energy conversion at middle and high temperatures up to 900°C. Though the thermoelectric figure of merit of iron disilicide falls behind that of $Si_{1-x}Ge_x$ which has already been applied to power generation in deep space probes,[5] $FeSi_2$ semiconductor has received attention from many workers because of its low cost, nontoxic character, high thermal stability, corrosion resistance and chemical stability.[3,4]

β-$FeSi_2$ is known to be a semiconducting material with orthorhombic structure, which is stable below about 970°C. The high temperature phase is metallic and eutectic, and consists of cubic FeSi (ε-phase) and tetragonal Fe_2Si_5 (α-phase). Consequently, it is absolutely necessary for a would-be good thermoelectric material to be completely transformed from the metallic phase to the semiconducting β-phase by annealing process.[6]

To improve the figure of merit, doping technique is desirable. Pure β-$FeSi_2$ is an intrinsic semiconductor, and n-type thermoelectric material is obtained by doping with Co or B and p-type one is obtained by Al or Mn.[3,4] Recently, many workers have tried to improve thermoelectric conversion efficiency of $FeSi_2$ by employing various preparation techniques. Matsubara et al.[7,8] reported that plasma (O_2 and SiH_4) treatment for $FeSi_2$ particles was very effective to enhance the electrical conductivity and Seebeck coefficient.

Though many workers have actively worked to improve the thermoelectric figure of merit of Fe-Si system, none of them has yet satisfactorily explained the transport mechanism which gives rise to thermoelectricity. Consequently, in this work, for the purpose of making clear the role of microstructure, that is, the effects of density and porosity in the thermoelectric properties of Fe-Si system, thermoelectric measurements and spectroscopic characterization have been conducted.

II. Experimental Procedure

1. Sample preparation and characterization

A commercial $FeSi_2$ powder (Cerac Inc., -20 mesh, 99.9% pure) was milled into fine particles using Y-TZP balls/alumina jar for 50 h. The average particle size of the obtained powder was 1.3 μm. The oxygen impurity introduced during 48 h milling process was analyzed to be approximately 0.64 wt% from the result of preliminary experiment.

The milled powder was press-formed into a compact (45×6×3~6 mm rectangular type) using a binder (5 wt% PVA solution), and sintered at 1160~1200°C in Ar+7%H_2 atmosphere. Various sintering times of 0~5 h were applied to control the density of the sintered specimens.

The density of each specimen measured by Archimedean method was 3.376~4.217 g/cm^3. This value is much lower than 5.132 g/cm^3, the theoretical density of α+ε phase.

Finally, a rectangular bar (10~15×3.3×4.5 mm) was cut off from the sintered specimen using a diamond saw to measure the thermoelectric properties, and was annealed at 865°C for 50 h and again at 800°C for 100 h under Ar+7%H_2 atmosphere to be transformed to the semiconducting β-phase.[9] Table 1 shows preparation conditions and densities of the specimens.

XRD measurements were carried out on the sintered and measured specimens using FeKα radiation to examine the phases present. Scanning electron microscope (SEM) and energy dispersive X-ray spectroscopy (EDS) observations, and oxygen-nitrogen analysis for the specimens were also conducted.

2. Measurement of thermoelectric property

Four grooves were put on a rectangular specimen. The heads of the two Pt-Pt13%Rh thermocouples were embedded in the drilled holes at the two ends of a specimen and they were held with Pt wires placed along the grooves. The electrical conductivity and thermoelectric power were measured simultaneously for the specimen at 50~700°C in Ar+7%H_2 atmosphere as shown in Fig. 1.

Electrical conductivity was measured using the d.c. four-probe technique. Ohm's law was always checked by changing the current value. The average voltage drop obtained from forward/reverse current directions was used to calculate the conductivity. For thermoelectric power measurements, a temperature gradient in the specimen was generated by heating one end of the specimen at temperatures below 200°C and blowing the cool air above 200°C. Plots of thermoelectric power against temperature difference showed a straight line in all cases, and the Seebeck coefficient was calculated from the slope.

III. Results and Discussion

1. Analyses of phase and microstructure

XRD analysis, as given in Fig. 2, shows that major

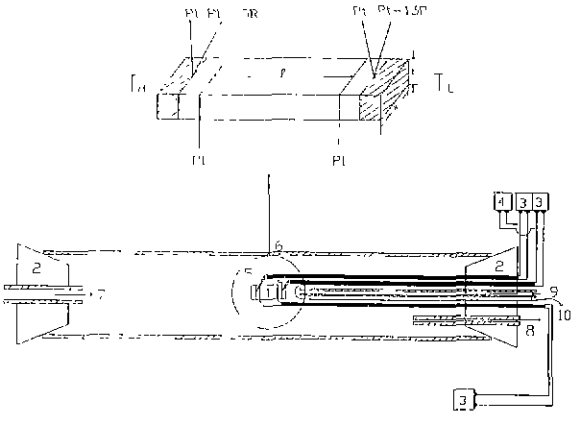

1 specimen
2 silicon rubber
3 voltmeter
4. DC constant current power supply
5 thermocouple
6 alumina tube
7 gas inlet
8 gas outlet
9 air inlet or sub-heating element
10 air outlet

Fig. 1. Schematic diagram of the apparatus for electrical conductivity and Seebeck coefficient measurement.

Table 1. Name, Condition of Preparation and Density of Specimens

sample	1160/2 h	1175/2 h	1190/2 h	1200/2 h	1190/0 h	1190/30 m	1190/1 h	1190/5 h
sintering temp. (°C)	1160	1175	1190	1200	1190	1190	1190	1190
sintering time (h)	2	2	2	2	0	0.5	1	5
density (g/cm^3)	3.5099	3.8249	4.2174	4.1423	3.3761	3.6068	3.7107	4.1567
relative density (%)	68.39	74.53	82.18	80.72	65 79	70.28	72.31	81.00
open porosity (%)	23.67	16.43	6.8	10.37	27.28	21.55	19.2	7.99

phases of the sintered specimens are α-Fe_2Si_5 and ε-FeSi. Fig. 3 shows XRD patterns of the annealed specimens. In spite of the long time annealing, the residual metallic phases were detected. It can be seen in Fig. 3 that the intensity of XRD peaks of ε-FeSi tends to decrease with increase in sintering time, that is, with increase in density, while that of α-Fe_2Si_5 makes little difference among them. The intensity of XRD peaks of ε-FeSi decreased with increase in sintering temperature, too. These results may lead to the following two possible explanations.

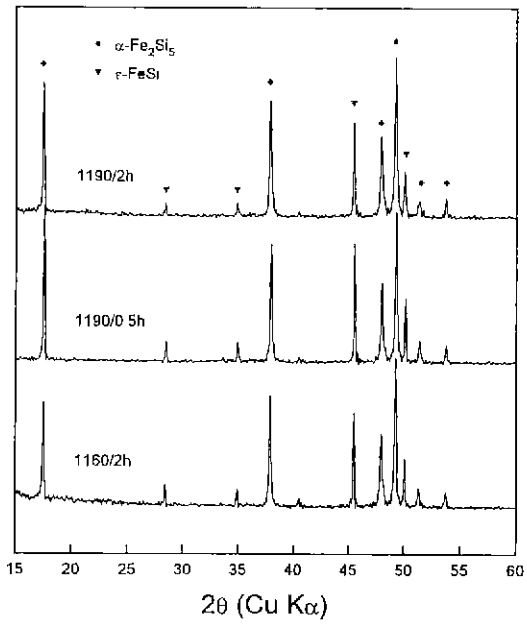

Fig. 2. XRD patterns of $FeSi_2$ specimens after sintering.

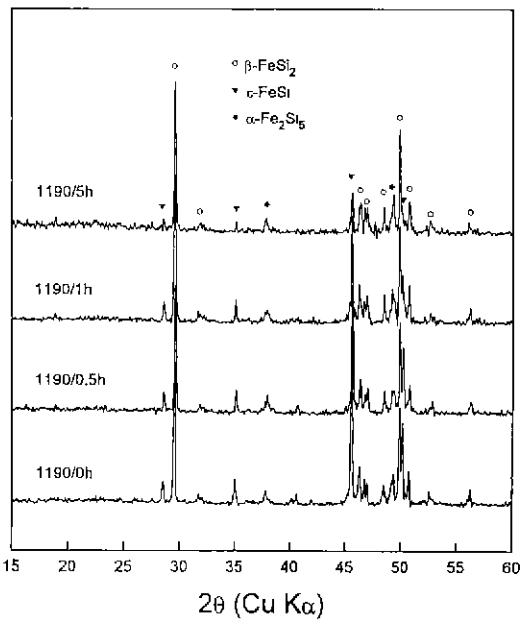

Fig. 3. XRD patterns of $FeSi_2$ specimens with various sintering times after annealing.

Firstly, it can be said that the phase transformation to β-phase more rapidly and effectively occurred with increasing density. Fig. 4 shows the variation in electrical conductivity of sintered specimens with annealing time. Two kinds of sintered specimens (1190°C/0.5 h, 1190°C/5 h) were used. The annealing time was varied while annealing temperature was fixed as 840°C, which was reported to be the effective temperature by Nishida et al.[3] It can be seen in Fig. 4 that the electrical conductivity of 1190/5 h specimen decreased abruptly and then was kept constant after 1 h of annealing. On the other hand, the electrical conductivity of 1190/0.5 h specimen was held constant after 3 h annealing. These results indicate that the phase transformation to β-phase occurs more rapidly in the specimens of the higher density rather than in those of the lower density. It can be also seen in Table 1 that the phase-to-phase contact area and the potential energy of the phase transformation may probably increase with increase in density of the specimen. However, it is assumed that the density had little effect upon the phase transformation velocity, since the total annealing time 150 h in this experiment, is enough to transform from the metallic phases (except isolated phases) to semiconducting β-phase.

Secondly, the residual unreacted metallic phases can be resulted from oxidation of the specimen during sintering and annealing. The phase transformation for Fe-Si system may occur by the following two kinds of reactions.[3,6] The decomposition reaction, α→β+Si occurs and then Si+ε→β follows below 850°C, and the peritectoid reaction, ε+α→β occurs above 860°C. Two-steps annealing was carried out in this work for the complete transformation. However, XRD patterns of α-Fe_2Si_5 made little difference and the intensity of XRD peaks of ε-FeSi increased with decrease in density, unexpectedly. This phenomenon can be seen in Fig. 5 from XRD intensity ratio of ε-FeSi to β-$FeSi_2$. It

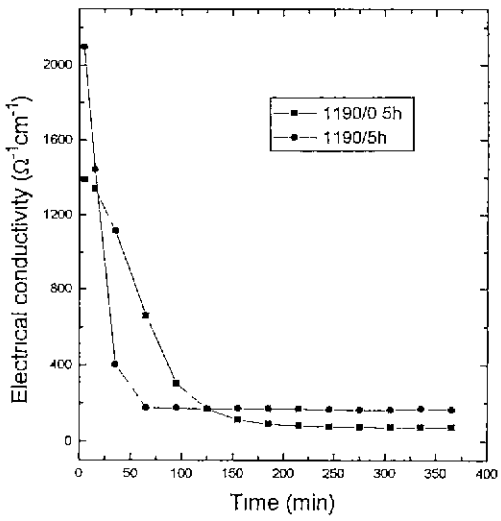

Fig. 4. Variation in electrical conductivity of sintered specimen with annealing time at 840°C.

is assumed that Si in matrix was probably oxidized by oxygen introduced during the process and hence a part of ε-FeSi phase could not react with Si and remained unreacted. Furthermore, it is considered that the surface area of the grains in the specimen increased with a decrease in density, and hence the grain-to-oxygen contact area increased and the residual ε-FeSi phase probably increased. This interpretation was confirmed by the oxygen content analysis. While the oxygen content of 1190/0 h specimen was 10.55 wt%, that of 1190/5 h specimen was 5.01 wt%. The obtained results are similar to that of plasma-processed β-$FeSi_2$ reported by Miki et al.[10]

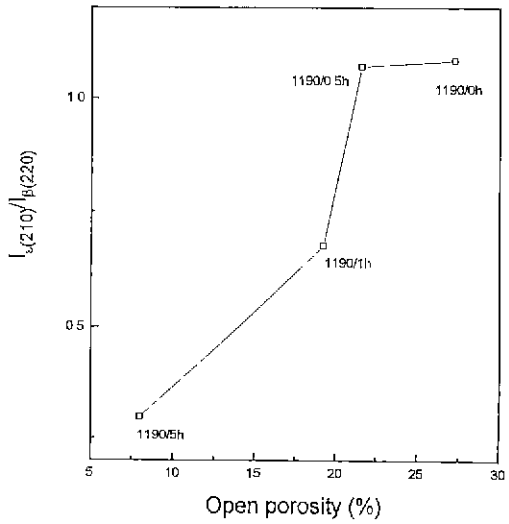

Fig. 5. XRD intensity ratio of ε-FeSi to β-$FeSi_2$ in specimens with various sintering times after annealing.

SEM photographs of the specimens are given in Fig. 6. It can be seen in Fig. 6 that the grain size increased and the pore portion decreased with increasing sintering temperature and time. It can be also seen in Fig. 6 that the whitish and dot-like phases exist in photographs of S (sintered)-1200/2 h specimen. The composition ratios of Si/Fe (at%) in matrix and whitish area of 1190/5 h specimen analyzed by EDS were 2.6 and 1.3, respectively, and the corresponding phases were assumed to be α-Fe_2Si_5 and ε-FeSi, respectively. However, since the dot-like phase was too small to be analyzed directly, its ratio can be estimated as 11.5 with negligible Fe element from the result of a preliminary experiment. Therefore, dot-like phases are considered to be an aggregated phase resulting from impurities

In SEM photographs of the annealed specimens, it can be seen that the fine reaction products exist at the grain-pore boundaries and aggregated phases boundaries. From

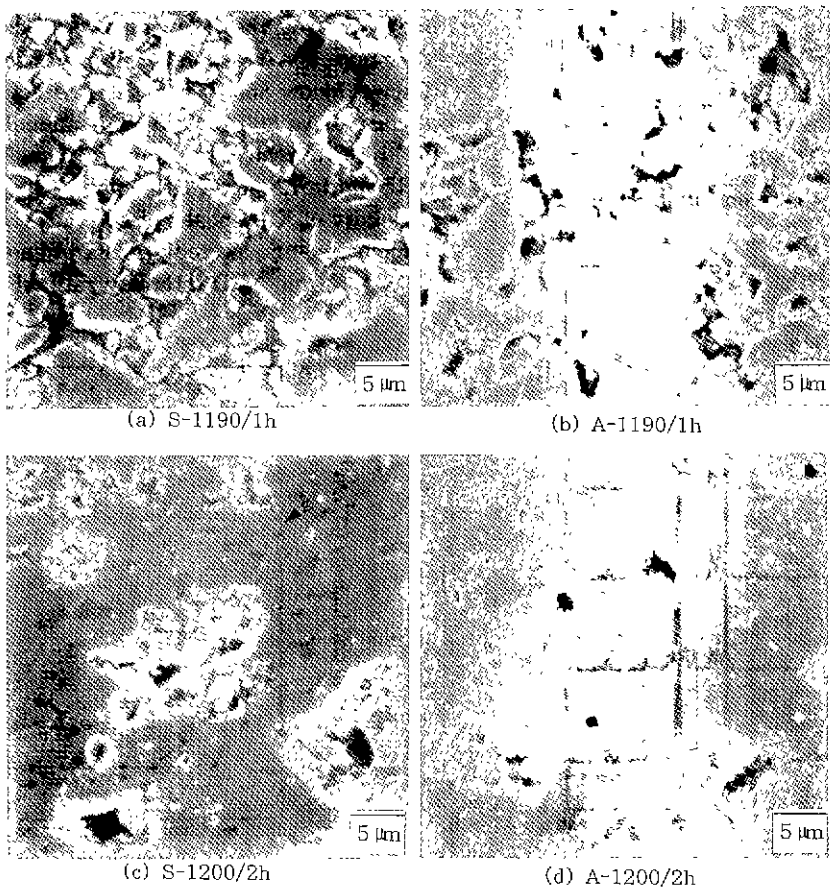

Fig. 6. SEM photographs of $FeSi_2$ specimens: (a), (c) after sintering, and (b), (d) after annealing.

EDS analysis on grain-pore boundary, Si/Fe and Si/O ratio for A(annealed)-1190/0 h specimen were 2.7 and 1.4, respectively. On the other hand, that for A-1190/5 h were 2.6 and 3.2, respectively. That is, the oxygen content of the lower dense specimen is larger than that of the higher dense specimen. This result well agrees with the tendency of oxygen content analysis. Although Si/Fe and Si/O ratios of ε-phase in A-1190/5 h specimen were 1.8 and 1.5, respectively, those of S-1190/5 h specimen were 1.3 and 3.2, respectively, that is, Si/O ratio increased when the specimen was annealed. This fact can be supported by the previous mention that Si resulting from the decomposition reaction is oxidized during the heat treatment, and hence ε-FeSi phase remains unreacted.

From the results of oxygen content analysis, EDS and XRD analysis, it is considered that the residual ε-FeSi phase in the annealed specimens is an unreacted phase resulting from oxidation. It is also considered that the lower dense specimen has the higher possibility of oxidation and hence contains the more oxygen content due to the produced oxides than the higher dense specimen. Therefore, the bump-like fine reaction products existing on pore/grain boundaries are assumed to be oxides resulted from silicon.

2. *Thermoelectric properties*

2.1 *Electrical conductivity*

The temperature dependence of the electrical conductivity for the specimens is shown in Figs. 7 and 8. The electrical conductivity increased exponentially with increasing temperature. The activation energy calculated from the slope of the electrical conductivities for all specimens at high temperature region (above about 300°C) was 0.452 eV. This indicates that the high temperature region seems to be an intrinsic region. This value is similar to that of p-type $FeSi_2$ (doped with Al), 0.45 eV, reported by Birkholtz et al.[11] On the other hand, the activation energy at low temperature region was varied from 0.197 to 0.086 eV. This result indicates that the low temperature region seems to be an extrinsic region caused by a newly formed acceptor level.[11]

It can be seen in Figs. 7 and 8 that the electrical conductivity was little affected by density. This result may be attributed to the fact that the residual metallic phase in the specimen of the lower density made compensation effect for the conduction loss by its electrical conductivity. The ratio of Si/Fe decreases with oxidation of Si in the matrix, and consequently Si-vacancies and acceptor levels may be produced and the quantity of ε-FeSi phase also increases, and hence the carrier density becomes higher, resulting in improvement of the electrical conductivity. It can be also seen in Figs. 7 and 8 that the electrical conductivities of the lower dense specimens (1190/0 h and 1160/2 h) are slightly higher than those of the higher dense specimens at about 300°C. This may be attributed to the increment of the carrier density resulting from the oxidation of Si. Generally speaking, however, the specimens of the higher density shows the higher electrical conductivity, probably because of the excessive grain growth.

2.2 *Seebeck coefficient*

The temperature dependence of the Seebeck coefficient for the specimens is shown in Fig. 9. The Seebeck coefficient for all samples exhibited p-type conduction caused by Si deficiency[10] in spite of non-doping. This deficiency is due to oxidation (because Si has more affinity to oxygen than Fe) and/or sublimation during sintering and annealing. The Seebeck coefficient of relatively higher dense specimens exhibited the maximum value at about 100~200°C, however, decreased abruptly with increasing

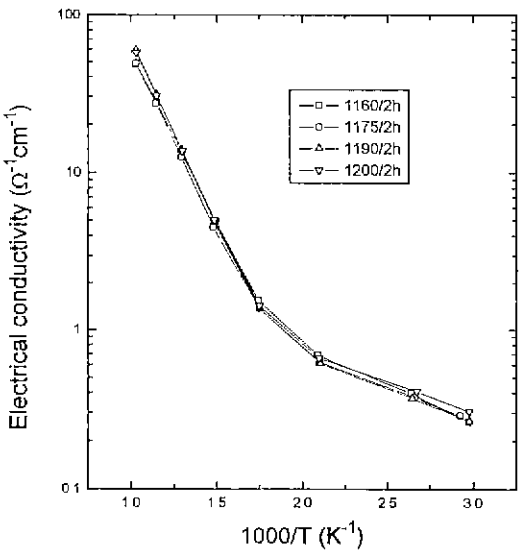

Fig. 7. Electrical conductivity of β-$FeSi_2$ with various sintering temperatures as a function of temperature.

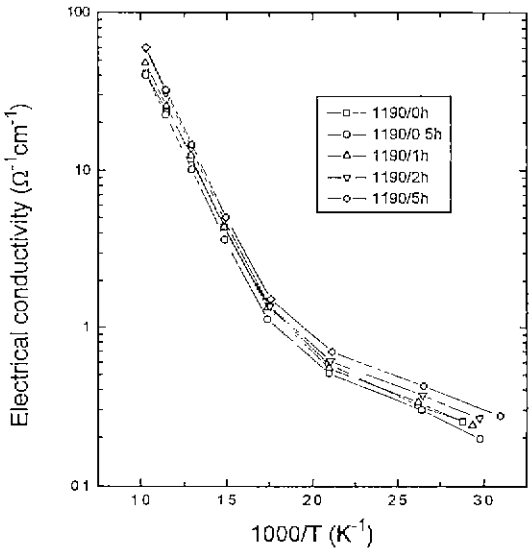

Fig. 8. Electrical conductivity of β-$FeSi_2$ with various sintering times as a function of temperature.

temperature up to about 400°C and then decreased gradually up to 700°C. The tendency of the lower dense specimens was similar to that of the higher dense specimens at large except for the temperatures below 100°C. Generally, above 400°C, the Seebeck coefficient of the lower dense specimens was higher than that of the higher dense specimens, and the tendency was reversed below 400°C. From the results of this work and Birkholtz et al.'s work,[11] the temperature dependence of the Seebeck coefficient can be divided into three regions; a sudden increase region (up to the maximum value), a sudden decrease region (up to about 400°C) and a gradual decrease region (above 400°C, intrinsic region).

Birkholtz et al.[11] reported a band-type conduction in p-type $FeSi_2$ and a hopping (small polaron)-type[12] conduction in n-type $FeSi_2$, and also reported that a theoretical band calculation for β-$FeSi_2$ made it possible to anticipate the strong electron-phonon interaction in the band edge states.[11,13] Accordingly, the band model was introduced to explain the results of this work.

Generally, a correlation between the electrical conductivity and Seebeck coefficient can be expressed as follows:[11]

$$\alpha = \pm \gamma \frac{k}{e}(K - \ln \sigma) \tag{2}$$

where γ is a factor which approaches to 1 with increase in carrier density and temperature, and K is a constant.

It can be seen in Figs. 7 and 8 that the electrical conductivity increases exponentially in the intrinsic region because of the conduction by both hole and electron. On the other hand, it can be seen in Fig. 9 that the Seebeck coefficient in this region decreases gradually because of bipolar effect,[14] and increases with decreasing density as well as electrical conductivity. In the case of non-doped

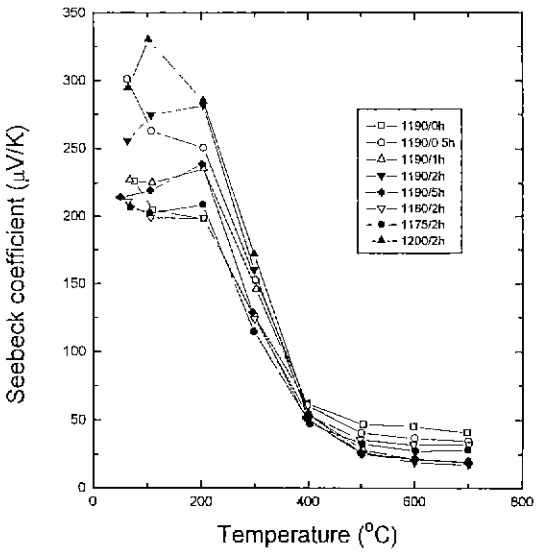

Fig. 9. Seebeck coefficient of β-$FeSi_2$ with various densities as a function of temperature.

β-$FeSi_2$ (with extremely low carrier density) as in this experiment, the intrinsic region can be expressed by a constant slope region, as given in Eq.(2).

However, a sudden decrease region is very difficult to explain. This region can be expressed as the exhaustion region of the extrinsic semiconductor caused by the acceptor level. In this region, the Seebeck coefficient for a single band conduction can be expressed as follows:[11]

$$\alpha = \frac{k}{e}(\delta + \ln \frac{N_v}{p}) = \frac{k}{e} \ln \frac{N_v e^{\delta}}{p} \tag{3}$$

where δ is the transport term, N_v the state density of valence band, p the density of hole. From the equation (3),

$$\ln \frac{N_v}{p} = -\frac{(E_F - E_v)}{kT} \tag{4}$$

can be obtained,[15] consequently, the Seebeck coefficient, α, varies with Fermi energy, E_F. Since this region is non-degenerate region[16] with a constant carrier density, the temperature dependence of E_F in this region is similar to that of the doped Ge.[15] As the quantity of the dopant increases, E_t decreases and is little affected by temperature.[16] Accordingly, if the exhaustion region caused by the dopant extends, this sudden decrease region should be extended to higher temperatures.

It can be seen in Fig. 9 that the Seebeck coefficient increases with increasing density at large. This is considered to be caused by the quantitative differences of ε-FeSi phase in specimens. As the metallic ε-FeSi phase increases, the electrical conductivity also increases, but the Seebeck coefficient decreases as Eq.(2) implies. It is also considered that Seebeck coefficient of the specimen of the lower density, generally, decreases because of non-stoichiometry by its feasibility of oxidation caused by its microstructural characteristics. From these results, it can be clearly explained that both the electrical conductivity and Seebeck coefficient are mutually in their reverse effects and they are mainly affected by the carrier density resulting from the residual metallic phase, ε-FeSi.

The decrease of Seebeck coefficient for the higher dense specimens below 100°C might be caused by the fact that Fermi level becomes gradually more adjacent to the valence band within the degenerate region. On the other hand, the degenerate temperature for the lower dense specimens might be moved to the lower temperature region, which was caused probably by a newly formed acceptor level.

2.3 Power factor

Fig. 10 shows the temperature dependence of power factor, $\sigma\alpha^2$, appropriated to evaluate the electrical property of thermoelectric materials. The power factor for all specimens exhibited the maximum value at about 200°C, which decreased with increasing temperature up to about 400°C (for the specimens of the lower density)

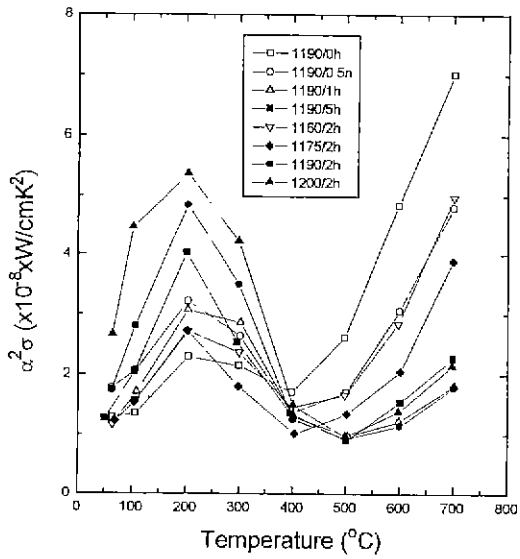

Fig. 10. Power factor of β-$FeSi_2$ with various densities as a function of temperature.

and 500°C (for the specimens of the higher density), and then increased again with temperature.

The power factor may be affected more by the Seebeck coefficient than the electrical conductivity. While the electrical conductivity of the lower dense specimens was improved in degenerate region (below 400°C), their Seebeck coefficient decreased, and hence the power factor decreased. Consequently, it can be seen that the residual metallic phase has an harmful effect on the power factor. On the other hand, since the carrier density increases exponentially with temperature in an intrinsic region (above 400°C), the increase in the carrier density caused by the residual metallic phase can be negligible. Therefore, the effect of microstructure is considered to be closely related to the power factor. Hence, more investigations are required to completely understand its effect. Accordingly, it is necessary to decrease electrical conductivity appropriately in order to improve power factor in the intrinsic region.

IV. Conclusions

The following conclusions can be drawn from the present study on the thermoelectric properties of $FeSi_2$ prepared by the conventional sintering process.

1. The residual metallic phases α-Fe_2Si_5 and ε-FeSi were detected by XRD analysis in spite of long time annealing. The intensity of the XRD peaks of ε-FeSi tended to increase with decrease in density of the specimen, while that of α-Fe_2Si_5 made little difference. Si in the matrix was possibly oxidized by oxygen introduced during the process and hence a part of ε-FeSi phase could not react with Si and remained unreacted. The oxidation was more remarkable in the specimen with the lower density.

2. The electrical conductivity of the specimen exhibited the typical semiconducting behavior. The activation energy in the intrinsic region (above about 300°C) was approximately 0.452 eV, and the activation energy at low temperature region (extrinsic region) was varied from 0.197 to 0.086 eV. The electrical conductivity was unexpectedly little affected by density. This is assumed to be the compensation effect caused by the metallic phase, ε-FeSi, for the conduction loss.

3. In spite of non-doping, the Seebeck coefficient for all specimens exhibited p-type conduction due to Si deficiency. The Seebeck coefficient of the specimen of relatively higher density exhibited the maximum value at about 100~200°C, and the value decreased abruptly with increasing temperature up to about 400°C (non-degenerate region) and then decreased gradually up to 700°C (in intrinsic region). The tendency of the lower dense specimens was similar to that of the higher dense specimens at large except for the temperatures below 100°C.

4. The power factor of all specimens exhibited the maximum value at about 200°C, and decreased with increasing temperature up to about 400 (for the lower dense specimens) and 500°C (for the higher dense specimens), and then increased again with temperature. The power factor is considered to be more affected by the Seebeck coefficient than the electrical conductivity. The effect of residual metallic phase was negligible in the intrinsic region.

References

1. D. M. Rowe, and C. M. Bhandari, "Modern Thermoelectrics," Holt, Rinehart and Winston, London, 1983.
2. K. Uemura, and I. Nishida, "Thermoelectric Semiconductors and Their Applications," Nikkan Shinbun Press, Tokyo, Japan, 33-37 (1988).
3. I. Nishida, K. Masumoto, M. Okato, and T. Kojima, "Formation of $FeSi_2$ from Sintered FeSi-Fe_2Si_5 Eutectic Alloys," *Trans. Jpn. Inst. Metals*, **26**(5), 369-374 (1985).
4. Y Isoda, T. Ohkoshi, I. Nishida, and H. Kaibe, "Si-composition and Thermoelectric Property of Mn and Co doped $FeSi_2$," *J. Mater. Sci. Soc. Jpn*, **25**(6). 311-319 (1989).
5 D. M. Rowe, G. Min, and Y. A. Chen, "Carrier Enhancement Mechanism in n-Type SiGe-GaP Alloys," *Proc., 12th ICTEC*, 69-73 (1993).
6. T. Kojima, M. Sakata, and Isida, "Study on the Formation of $Fe_{1-x}MnxSi_2$ from the Sintered FeSi-Fe_2Si_5 Eutectic Alloy Doped with Manganese," *J. Less-Comm. Metals*, **162**, 39-49 (1990).
7 K. Matsubara, and T Koyanagi, "Amorphous $FeSi_2$ Films As a New Thermoelectric Material Prepared by Ionized-Cluster Beam(ICB) Technique," *Proc., 6th ICTEC*, 1-6 (1986).
8. K. Matsubara, T. Miki, K Nagao, K. Kishimoto, O. Nakanshi, O. Ueda, and K. Fujii, "Characterization and Thermoelectric Properties of New -$FeSi_2$ Ceramics Developed by Rf-Plasma Processing in O_2 and SiH_4 Gases,"

Proc., 11th ICTEC, 24-27 (1992).
9. T. Sakato, Y. Sakai, H. Yoshino, H. Fujii, and I. Nishida, "Studies on the Formation of $FeSi_2$ from the FeSi-Fe_2Si_5 Eutectic," *J. Less-Comm. Metals*, **61**, 301-303 (1978).
10. T. Miki, Y. Matsui, K. Matsubara, K. Kishimoto, K. Nagao, and I. Fujji, "Point Defects in Plasma-Processed β-Iron Disilicide Ceramics," *Proc., 12th ICTEC*, 29-33 (1993).
11. U. Birkholtz, and J. Schelm, "Mechanism of Electrical Conduction in β-$FeSi_2$," *Phys. Stat. Sol.*, **27**, 413-425 (1968).
12. I. Shiota, Y. Isoda, Y. Shinohara, Y. Imai, and I Nisida, "Semiconducting and Thermoelectric Properties of Iron Disilicides Doped with Aluminum," *Proc., 2th ICTEC*, 151-154 (1993).
13. T. Kojima, M. Okamoto, and I. Nishida, "Semiconducting and Thermoelectric Properties of Sintered Iron Disilicide," *Proc., 5th ICTEC*, 56-61 (1984).
14. H. J. Goldsmid, "Thermoelectric Refrigeration," Plenum Press, New York, 1964.
15. L. V. Azaroff, and J. J. Brophy, "Electronic Processes in Materials," pp. 207-210, McGraw-Hill Inc., New York, 1963.
16. R. F. Pierret, and W. Neudeck, "Modular Series on Solid State Devices," **6**, 91-133, Addison-Wesley Pub. Co., (1989).